Anisotropy of spin polarization and spin accumulation in Si/Al_2O_3/ferromagnet tunnel devices

S. Sharma,[1,2] S. P. Dash,[3] H. Saito,[1] S. Yuasa,[1] B. J. van Wees,[2] and R. Jansen[1]

[1]*National Institute of Advanced Industrial Science and Technology (AIST), Spintronics Research Center, Tsukuba, Ibaraki, 305-8568, Japan*

[2]*Zernike Institute for Advanced Materials, Physiscs of Nanodevices, University of Groningen, 9747 AG, Groningen, The Netherlands*

[3]*Department of Microtechnology and Nanoscience, Chalmers University of Technology, SE-41296, Göteborg, Sweden*

(Received 3 June 2012; revised manuscript received 11 August 2012; published 8 October 2012)

The contribution of the spin accumulation to tunneling anisotropy in Si/Al_2O_3/ferromagnet devices was investigated. Rotation of the magnetization of the ferromagnet from in-plane to perpendicular to the tunnel interface reveals a tunneling anisotropy that depends on the type of the ferromagnet (Fe or Ni) and on the doping of the Si (n or p type). Analysis shows that different contributions to the anisotropy coexist. Besides the regular tunneling anisotropic magnetoresistance, we identify a contribution due to anisotropy of the tunnel spin polarization of the oxide/ferromagnet interface. This causes the spin accumulation to be anisotropic, i.e., dependent on the absolute orientation of the magnetization of the ferromagnet.

DOI: 10.1103/PhysRevB.86.165308 PACS number(s): 72.25.Hg, 72.25.Dc, 73.40.Gk, 85.75.−d

I. INTRODUCTION

In a magnetic tunnel junction (MTJ) with two ferromagnetic (FM) electrodes, a large change in resistance can be produced when the relative alignment of the magnetization of the two magnetic layers is switched.[1] The resulting tunneling magnetoresistance (TMR) depends on the tunnel spin polarization (TSP).[2] Also, it has been observed that in a tunnel junction with a single FM layer,[3] a change in tunnel resistance occurs when the magnetization of the magnetic layer is rotated and the absolute orientation of the magnetization changes. This phenomenon is called tunneling anisotropic magnetoresistance (TAMR). Depending upon the device configuration, TAMR can be classified as in-plane and out-of-plane TAMR. The in-plane[3–7] TAMR refers to the change in tunnel resistance when the magnetization is rotated in the plane of the magnetic layer. On the other hand, out-of-plane[2,5,8–10] TAMR refers to the change in tunneling resistance when the magnetization is rotated from in-plane to out-of-plane.

Theoretical investigations reveal[11] that the TAMR phenomenon is generic in transition metal FMs. For Co, these calculations predict an anisotropy in tunneling density of states (DOS) ranging from 0.3–1.3%. This is supported by the relatively small TAMR value (below 0.5 %) in MTJs with one transition metal electrode,[4] consistent with the weak spin-orbit coupling (SOC) in Fe or CoFe. One may expect that engineering the interface adjacent to tunnel barrier can improve the TAMR. For CoPt film, the anisotropy in tunneling DOS was predicted[11] to be $>12\%$. This was confirmed[8] by exploiting the enhanced SOC at the interface with CoPt based electrodes giving rise to large TAMR of 15%. Although the TAMR effect may be small in magnitude in tunnel contacts with transition metal FMs, it may influence the spin injection from a FM into a semiconductor (SC). Therefore, to correctly interpret the results of spin injection into a SC,[7,10] it is essential to investigate the TAMR effect in tunnel contacts with a SC.

The recent breakthrough[12,13] in electrical injection and detection of the spin-polarized carriers in Si at 300 K has given a boost to the research activities in silicon spintronics.[14–17] Several control experiments[18,19] have proven unambiguously that the large room-temperature spin signal is genuine and originates from the spin-polarized tunneling and the spin accumulation in the Si bands. This now enables the systematic study of the various parameters that influence the spin injection into silicon,[20] of which our understanding is still rather limited. A feature that provides more insight is the anisotropy of the tunnel conductance, which may have various sources, including the TAMR. Previous reports on TAMR concluded that the change in tunnel resistance is due to the anisotropy in DOS[3–5,8,9,11,21] at the tunnel interface between a FM and an insulating barrier. As the magnetization direction is rotated, it faces different DOS, thereby changing the transport across the tunnel contact. This leads to the change in resistance of the tunnel contact. Other sources of the anisotropy include the anisotropic tunnel spin polarization (TASP) associated with the ferromagnet/tunnel barrier interface[22,23] and/or anisotropic spin relaxation time τ_s inside the nonmagnetic SC. Such an anisotropic spin relaxation has been invoked to describe experiments with graphene,[24] where it was argued that there is 20% decrease in spin-relaxation time for electrons with spin perpendicular to the graphene layer compared to the spins oriented parallel to the layer. Assuming the TSP to be isotropic, the anisotropy in τ_s will results in anisotropic spin accumulation $\Delta\mu$ inside the semiconductor. On the other hand, the anisotropic TSP of the magnetic tunnel contact will also create different spin accumulation levels inside the SC, irrespective of the anisotropy in τ_s. The anisotropic spin accumulation in a SC, caused by either the anisotropy of TSP or by the anisotropic spin relaxation time in a SC, makes the measured signal to be anisotropic. Distinguishing between these different sources of the anisotropy is essential for the correct interpretation of the data.

In the present work, using tunnel contacts made on n-type as well as on p-type Si with Fe or Ni electrodes, we have been able to separate the different sources of the tunneling anisotropy. Rotation of the magnetization of the ferromagnet in a plane perpendicular to the magnetic layer results in an out-of-plane tunneling anisotropy that depends on the type of ferromagnet and on the doping of the Si (n and p type). Analysis reveals that different contributions to the tunneling anisotropy coexist. In addition to regular TAMR, we identify a contribution due to anisotropy of the TSP. This causes the injected spin accumulation in Si to be dependent on the absolute orientation of the magnetization of the ferromagnet. Further, we observed

that due to magnetic shape anisotropy of the magnetic layer, the magnetization makes an angle θ with the external field. This angular separation between the magnetization and the field is larger for Fe (saturation magnetization $M_S = 2.15$ T) compared to Ni ($M_S = 0.6$ T). The misalignment between the magnetization and the external field results in Hanle spin precession,[25] and it is more pronounced in the tunnel contacts with Fe compared to Ni. The relative strength of the different contributions to the anisotropy is found to depend on bias voltage. As a result, a significant change in the angular variation of the signal with bias voltage is observed, particularly for the tunnel contacts with Fe, while in the tunnel contacts with Ni, the measured signal retains its shape irrespective of the bias voltage.

This article is organized as follows. Section II A describes the device fabrication procedure along with the experimental technique used for characterizing the anisotropy of the tunnel resistance. This section also provides a brief introduction to the different components in the measured signal. In Sec. III, a detailed description of the experimental results obtained on the tunnel contacts with different ferromagnetic electrodes and different Si (n and p type) is given. This is followed by Sec. IV, describing the anisotropy of the spin accumulation in Si. This section includes detailed discussion about the Hanle spin precession, which arises from the misalignment between the magnetization and the external field. We also describe the fitting equation along with the strategy adopted for interpretation of the experimental results. A summary shall be presented in Sec. V.

II. EXPERIMENTAL PROCEDURE

A. Device fabrication

The tunnel contacts with different ferromagnets (Fe and Ni) were prepared on crystalline n-type (n) and p-type (p) silicon-on-insulator (SOI) wafers as described by Dash *et al.*[12] The carrier density measured at 300 K was found to be 1.8×10^{19} cm^{-3} (4.8×10^{18} cm^{-3}) for n (p) silicon. Initially, 300-nm SiO_2 was grown at 1150 °C on SOI wafers. The oxide was then patterned using standard optical lithography followed by wet etching to define the contact holes of area 100×200 μm^2 through SiO_2. After etching, the silicon substrates were introduced into the vacuum chamber and then Al_2O_3 was deposited. After that, a plasma oxidation was carried out for 2.5 min, which is considered to compensate for oxygen vacancies occurred during electron-beam evaporation of the Al_2O_3. Subsequently, the ferromagnetic electrode and the gold cap layer were deposited at a base pressure of 10^{-10} Torr followed by sputter deposition of the Cr/Au contact layers. It should be noted that the resulting aluminium oxide barrier and ferromagnetic electrodes were found to be amorphous and polycrystalline, respectively.

B. Measurement technique

The magnetotransport measurements have been carried out at 300 K in a system equipped with a sample rotator and a superconducting magnet. Two types of measurements, namely the field scan and the angle scan, were performed. The field scan measurements are obtained by fixing the angle ϕ between the applied field and the surface normal [see Fig. (1)] and varying the field strength. The ϕ values of 0°, 180°, and 360° correspond to the magnetic field perpendicular to the film plane, whereas 90° and 270° represent the field in the plane of the FM layer. The easy axis of the magnetization lies in-plane of the magnetic layer, i.e., along the X direction in Fig. 1. Sweeping the magnetic field with direction perpendicular to the tunnel interface (i.e., $\phi = 0°$, 180°, and 360°) and the magnetization lying along the easy axis, give rise to a Hanle curve.[12] On the other hand, sweeping the magnetic field with direction parallel to the tunnel interface and magnetization still lying along the easy axis (i.e., $\phi = 90°$ and 270°) results in an inverted Hanle curve.[20]

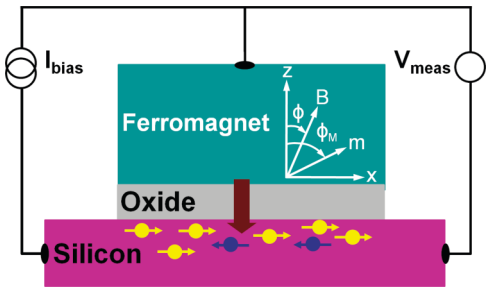

FIG. 1. (Color online) Schematic of the three-terminal geometry used for measuring the anisotropy in tunneling resistance. A constant current (I_{bias}), across the tunnel junction produces a voltage that changes when the magnetization of the magnetic layer is rotated out-of-plane. Here, ϕ represents the angle between a surface normal and the external field, whereas ϕ_M is the angle between the surface normal and the magnetization direction $\vec{m}$. Here, X and Z denote the in-plane and surface normal direction, respectively. The measured voltage V_{meas}, and therefore the tunnel resistance $R(\phi) = V_{\text{meas}}/I_{\text{bias}}$ depends on the magnetization direction.

In the angle scan, the sample is rotated, i.e., changing ϕ at a fixed external magnetic field B of 50 kOe. This is equivalent to rotating the magnetization from in-plane to out-of-plane. The experimental geometry is shown in Fig. 1. A constant current I_{bias} is sourced across the tunnel contact and the resulting voltage change (or dc resistance change) is measured as a function of angle ϕ when the magnetization of the magnetic layer is rotated. Due to a shape anisotropy (see Sec. IV for details), the magnetization of the magnetic layer makes an angle $\theta = (\phi_M - \phi)$ with applied field as shown in Fig. 1. Here, ϕ_M is the angle between the magnetization direction ($\vec{m}$) and the normal to the surface (Z axis).

In three-terminal configuration, a fixed source current across the junction results in a bias voltage $V = V_{\text{Si}} - V_{\text{FM}}$ such that for $V > 0$ (<0) spin-polarized electrons are injected in to (extracted from) the Si. The total voltage across the contact at constant current is given by $V_{\text{meas}} = V_0 + V_{\text{TAMR}}(\phi) + V_{\text{ASA}}(\Delta\mu(\phi))$, where V_0 is a constant voltage independent of the field and the other two terms describe the changes of the voltage produced when the magnetization of the magnetic layer is rotated. The second term V_{TAMR} is due to the tunneling anisotropic magnetoresistance[2] that comes from an anisotropy in spin tunneling due to Bychkov-Rashba[26] (BR) type spin-orbit interaction at the tunnel interfaces and/or intrinsic SOC in the ferromagnet.[3,4,11] The third term V_{ASA} is due to an anisotropic spin accumulation (ASA) in the Si, i.e., a

spin accumulation $\Delta\mu$ that depends on ϕ. This, in turn causes an angular dependence of V_{meas} across the junction, because V_{meas} is proportional to $\Delta\mu$.[12,13,20] An ASA may results from an anisotropic spin-relaxation time (τ_s) in the Si, from Hanle precession of spins in Si (due to the fact that the magnetization makes an angle θ with the external field) or due to tunneling anisotropic spin polarization.[2,22,23]

III. EXPERIMENTAL RESULTS

Two sets of tunnel contacts, respectively, made on n and p-type Si with Fe and Ni electrode were investigated. Below, we describe the experimental data obtained on the tunnel contacts with Fe (see Sec. III A) and Ni (see Sec. III B).

A. Tunnel contacts with Fe

Figures 2(a) and 2(b) show the field scan and the angle scan data for an Fe/Al_2O_3/p-Si tunnel contact taken at a constant current of -91.3 μA (hole injection into Si). A constant voltage $V_0 = -172$ mV was subtracted from the data. The red (blue) curve is obtained for $\phi = 0^\circ$ (90°) so that the external field is perpendicular (parallel) to the tunnel interface.

For the red curve, the observed symmetric Lorentzian peak around zero field is the signature of the Hanle effect.[12,13] At zero external field, there is no spin precession and the spin accumulation is maximum. With increasing external field, spins start to precess and the spin signal reduces to zero. At a field around 10 kOe, the curve (red) rises and after reaching a maximum above a field of $\approx$22 kOe, it saturates at this level. The rise in the signal is due to the rotation of the magnetization of the FM electrode. Above a field of $\approx$22 kOe, corresponding to the saturation magnetization of the Fe, the magnetization of the magnetic layer is aligned with the perpendicular field. The spins injected into the SC are then oriented parallel to the external field, and thus there is no precession. As a result of this complete alignment, the spin signal reaches a maximum and saturates.

The blue curve is obtained for $\phi = 90^\circ$ so that the external field is parallel to the tunnel interface. In this case, the spins injected into silicon will have orientation parallel to the external field and ideally there is no spin precession. Based on this, we expect a constant signal (no variation with B field) under steady-state conditions. However, we see that there is a dip in blue curve around zero field. The spin signal has a minimum at zero field, and as the external field is increased, the signal rises to the maximum value. This is referred as an inverted Hanle effect.[20] The suppression of the signal around zero field is attributed to the spin precession in magneto static fields, arising from roughness of the magnetic layer.[20]

We find that at sufficiently large field (>22 kOe) when the external field and the magnetization of the FM are aligned with each other, the Hanle and inverted Hanle curves [see Fig. 2(a)] do not saturate at same level. This indicates that the tunnel resistance [$R(\phi) = V_{meas}/I_{bias}$] depends on the absolute orientation of the magnetization of the FM electrode. To explore this fact in more detail, we have carried out an angular dependence study of the tunneling resistance. Figure 2(b) shows such a measurement for p-Si/Al_2O_3/Fe junction at $V = -172$ mV (hole injection into p-Si). By keeping the current fixed and changing the field angle ϕ, the curve in Fig. 2(b) is obtained. Comparison between Figs. 2(a) and 2(b) reveals that the angle scan reproduces the anisotropy observed between the two measurements of the Hanle and inverted Hanle effect. Defining the zero of the signal at $\phi = 0^\circ$, it raises to a value set by the in-plane ($\phi = 90^\circ$) signal, resulting in the twofold symmetry. Note that the curve is not sinusoidal.

Figures 2(c) and 2(d) show a similar data set for Si/Al_2O_3/Fe tunnel contacts with n-type Si at a bias of -172 mV (-807 μA). Similar to p-Si in Fig. 2(a), we obtain a symmetric Hanle and inverted Hanle curves around the zero field. For the

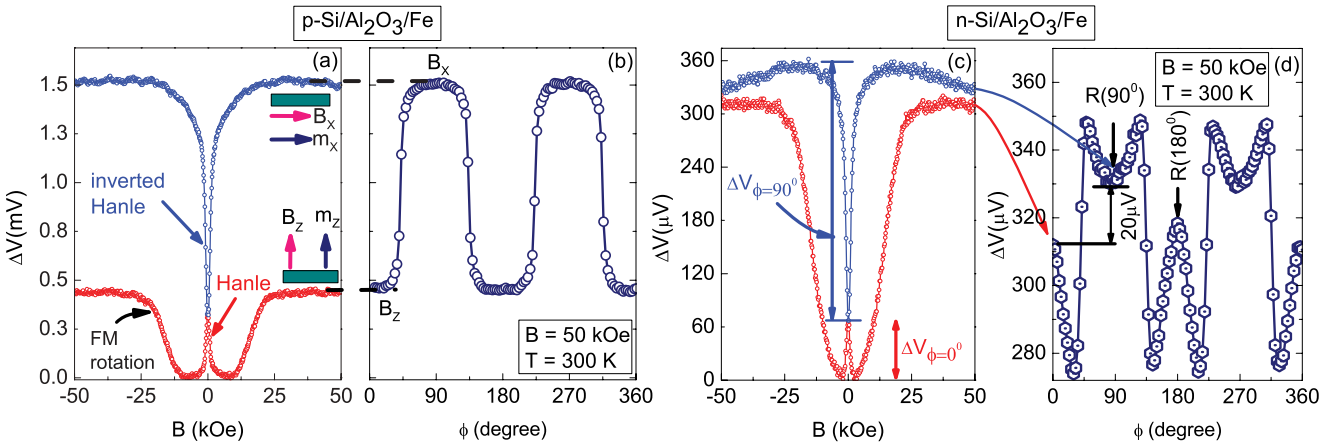

FIG. 2. (Color online) Experimental data for a p-Si/Al_2O_3/Fe junction (a) with field perpendicular (Hanle, red) and parallel to the tunnel interface (inverted Hanle, blue) and (b) the angular dependence of the measured signal at the same bias current ($I_{bias} = -91.3$ μA). Data are shown after subtracting an offset signal of $V_0 = -172$ mV. Labels B_X and B_Z in (b) represent the situations when the external field is parallel or perpendicular to the tunnel interface. Similar data set with n-Si/Al_2O_3/Fe tunnel contacts for (c) Hanle ($\phi = 0^\circ$, red), inverted Hanle ($\phi = 90^\circ$, blue) and (d) angle scan measurements at a bias voltage of -172 mV (-807 μA). In (c), $\Delta V_{\phi=0^\circ}$ and $\Delta V_{\phi=90^\circ}$ are the signal amplitude obtained in Hanle and inverted Hanle measurements respectively. In (d), $R(\phi)$ is the resistance (V_{meas}/I_{bias}) at the respective ϕ value. All the measurements have been performed at 300 K. Note that (c) and (d) have different vertical scales.

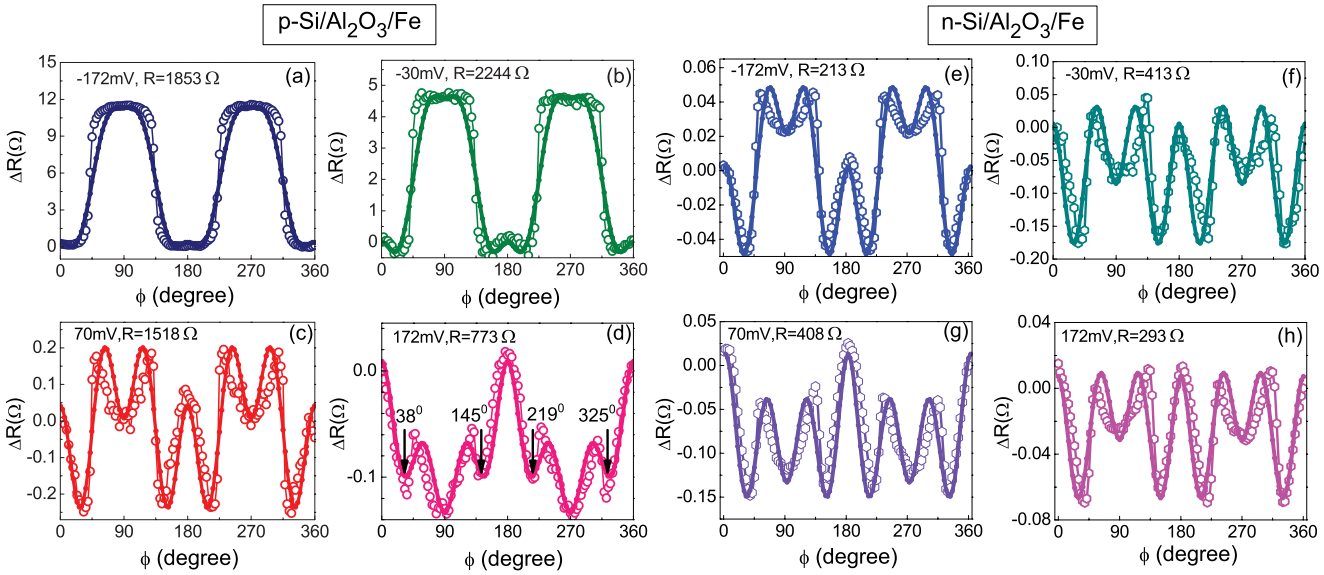

FIG. 3. (Color online) $\Delta R = R(\phi) - R_{\min}$ (where $R_{\min}$ is the minimum resistance) as a function of the field angle ϕ at -172 mV (a), -30 mV (b), 70 mv (c), and 172 mV (d), for p-Si/Al_2O_3/Fe. Similarly ΔR vs ϕ at -172 mV (e), -30 mV (f), 70 mv (g), and 172 mV (h), for n-Si/Al_2O_3/Fe tunnel contacts. The junction resistance values at each bias are indicated in each panel. Measurements have been taken on tunnel contacts at a field of 50 kOe and a temperature of 300 K. Note the different vertical scales for ΔR in each plot. Solid lines are fits using Eq. (4) in text.

Hanle curve, the signal reduces with increasing field. Then due to rotation of the magnetization of the FM, the signal rises until the external field reaches the saturation magnetization of the Fe. Beyond that the signal stays almost constant, as there is no spin precession in the silicon. In Fig. 2(c), $\Delta V_{\phi=0^\circ}$ and $\Delta V_{\phi=90^\circ}$ represent the signal amplitude for Hanle and inverted Hanle measurements. The net spin signal is proportional to $(\Delta V_{\phi=0^\circ} + \Delta V_{\phi=90^\circ})$. It represents the signal amplitude between two extreme situations. In the first situation, the magnetization lies in the plane of the magnetic layer and the spin signal corresponding to the spins injected into the silicon is zero due to spin precession (minimum in the Hanle curve). For the second situation, the magnetization still lies in the plane of the magnetic layer but the spin signal is maximum, as the spins injected into the silicon have orientation parallel to the field and do not precess (maximum in the inverted Hanle curve). At 50 kOe in Fig. 2(c), Hanle (red, $\phi = 0^\circ$) and inverted Hanle (blue, $\phi = 90^\circ$) curves are separated by $\approx$20 μV. This value is similar in magnitude to the signal obtained in the angle scan [see Fig. 2(d)] between $\phi = 0^\circ$ and 90°. We note that for the same bias voltage and field, the tunnel contact with n-Si has smaller anisotropy compared to those on p-Si. In addition, the measured signal in the angle scan has minima at $\phi = 90^\circ, 270^\circ$ and maxima at 0°, 180°, and 360° for tunnel contacts with n-Si. The angle scans in Figs. 2(b) and 2(d) indicate that V_{meas} departs from the expected $\cos(\phi)$ variation, implying that signals with different origin coexist.

In Fig. 3, we present the bias variation of anisotropic tunneling resistance for the tunnel contacts with Fe on p-Si [see Figs. 3(a)–3(d)] and n-Si [see Figs. 3(e)–3(h)]. The measured resistance at -172 mV in Fig. 3(a) displays two-fold symmetry with nearly square peaks at $\phi = 90^\circ$ and 270°. At -30 mV [see Fig. 3(b)], the resistance at $\phi = 90^\circ$ and 270° decreases whereas at 0° and 180° it starts to rise compared to minimum value. It becomes more clear in Fig. 3(c) at 70 mV for which the resistances at 90° and 270° are no longer the maximum, while at 172 mV in Fig. 3(d) it has become the minimum. The symmetry is no longer two-fold and the highest resistance is found for 0° and 180°. New features with minima approximately at 38°, 145°, 219°, and 325° can be seen in Figs. 3(c) and 3(d) at 70 and 172 mV, respectively. Also note that the amplitude of the signal decreases from negative to positive voltage.

The tunnel contact with n-Si [see Figs. 3(e)–3(h)] has local minima at 90°, 270°, and local maxima at 0°, 180°, and 360° within the investigated bias range. However, four minima positions are observed at the same angle for n-Si and p-Si, i.e., 39°, 147°, 219°, and 330°. The overall shape of the curves for n-Si [see Figs. 3(e)–3(h)] has little dependence on bias voltage [as opposed to p type, see Figs. 3(a)–3(d)].

B. Tunnel contacts with Ni

Next, we will describe the field scan along with the angle scan measurements on tunnel contacts with Ni electrode. Considering the low saturation magnetization ($M_s = 0.6$ T) for Ni and the fact that tunnel contacts with Ni have lower Hanle linewidth,[20] Figs. 4(a) and 4(c) display the data only up to 10 kOe for clarity. In Fig. 4(a), Hanle (red) and inverted Hanle (blue) measurements for p-Si/Al_2O_3/Ni tunnel contacts at -172 mV (hole injection in to p-Si) are shown. The voltage ΔV has been obtained after subtracting a constant voltage $V_0 = -172$ mV. The Hanle curve has a very sharp peak at zero field. Around 0.5 kOe, the signal rises very fast due to rotation of magnetization of the Ni layer. A change in the slope of the signal occurred around 6 kOe and it stays constant with further increase in field. The inverted Hanle curve (blue) has a dip around zero field and saturates at high magnetic field. In

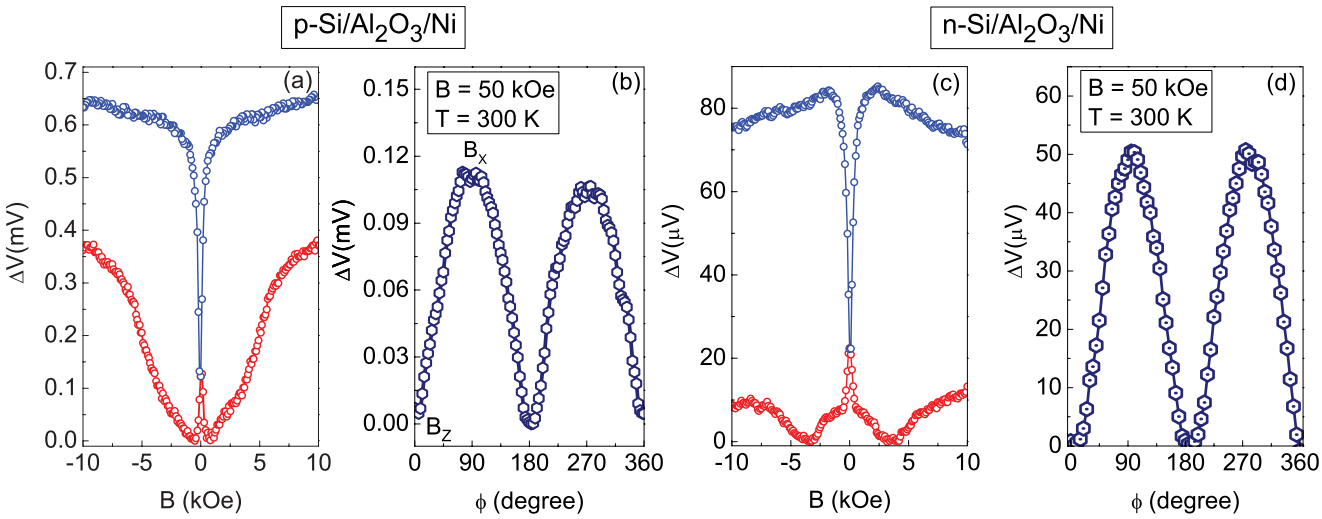

FIG. 4. (Color online) Experimental data for a p-Si/Al_2O_3/Ni tunnel contact (a) with field perpendicular (Hanle, red), and parallel to the tunnel interface (inverted Hanle, blue) and (b) angular dependence of the measured signal at a bias of -172 mV (-171 μA). Similar data set for n-Si/Al_2O_3/Ni tunnel contact are shown in (c), Hanle (red), inverted Hanle (blue), and (d) angular dependence of the measured signal at a bias of -172 mV (-650 μA). Data are shown after subtracting different offset voltages. In (b) and (d), a field with constant magnitude of 50 kOe is applied.

Fig. 4(b), the angle scan at 50 kOe and a bias of -172 mV gives cos(ϕ) variation of $\Delta V = V_{\rm meas} - V_0$ versus ϕ, with two maxima at $\phi = 90^\circ$ and 270°.

Figure 4(c) shows Hanle and inverted Hanle curves for n-Si/Al_2O_3/Ni tunnel contacts up to 10 kOe. We obtain a sharp Hanle peak around zero field, and with further increase in the field, the signal saturates at $\approx$7 kOe. For a field applied parallel to the tunnel interface, we observe the inverted Hanle effect with a dip in the signal around zero field and recovery of the signal at high field. In Fig. 4(d), the angle scan at 50 kOe and at a bias of -172 mV gives a cos(ϕ) variation with two maxima at $\phi = 90^\circ$ and 270°, similar to tunnel contact with Ni on p-Si.

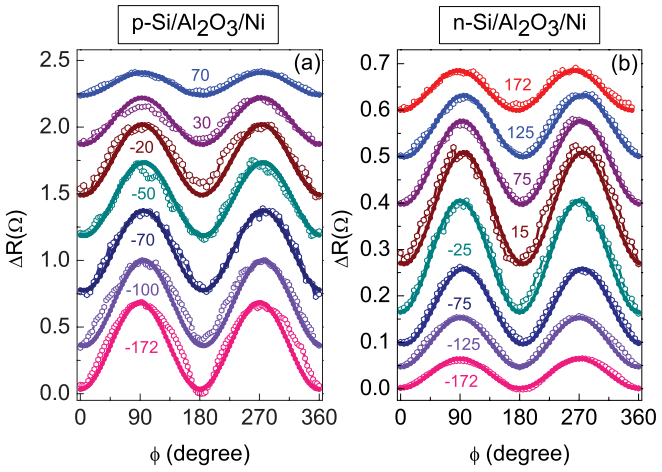

FIG. 5. (Color online) ΔR as a function of field angle ϕ for (a) p-Si/Al_2O_3/Ni and (b) n-Si/Al_2O_3/Ni tunnel junctions at bias voltages (in mV) indicated in each panel. The vertical axis is $\Delta R = R(\phi) - R_{\rm min}$, where $R_{\rm min}$ is the minimum resistance value. Solid lines are fits obtained through Eq. (4) in the text. Data are displaced vertically for clarity. All the measurements have been performed at 300 K and a field of 50 kOe.

The detailed bias dependence of anisotropic tunnel resistance for tunnel contacts on p and n-Si with Ni is shown in Figs. 5(a) and 5(b). The shape of the signal and twofold symmetry along 90° and 270° do not change with bias voltage. However, the magnitude of the total signal decays with increasing bias voltage. Figure 5(b) contains similar data set for n-Si/Al_2O_3/Ni tunnel contacts. Irrespective of the bias voltage, we have a cos(ϕ) variation with twofold symmetry along $\phi = 90^\circ$ and 270°. Note that this behavior is completely different from tunnel contacts with Fe (see Fig. 3). We will have a more detailed discussion of this topic in the next section.

C. Tunneling anisotropy and spin resistance versus bias voltage

1. *Tunnel contacts with Fe*

So far, we have shown the angular variation of the tunneling resistance at different bias voltages for different tunnel contacts (on n- and p-Si) with Fe and Ni. To gain insight, we define the tunneling anisotropy as $[(R_{\phi=90^\circ} - R_{\phi=180^\circ})/R_{\phi=180^\circ}]\times 100\%$, where $R(\phi)$ [see Fig. 2(d)] corresponds to the resistance values at angle $\phi = 90^\circ$ and 180°. Angles $\phi = 90^\circ$ and 180° represent the in-plane and out-of-plane orientation of the field, respectively.

Figure 6(a) shows the tunneling anisotropy of the p-Si/Al_2O_3/Fe junction as a function of bias voltage. At negative bias (hole injection), we see that the anisotropy is maximum and that it decreases linearly by going towards positive bias. Along positive bias (hole extraction), the anisotropy becomes negative and does not decay much. Figure 6(b) shows the variation of the spin resistance with bias voltage for the same tunnel junction. The spin resistance is defined as $\Delta R_{\rm spin} = [\Delta V_{B_{\phi=0^\circ}} + \Delta V_{B_{\phi=90^\circ}}]/I_{\rm bias}$, where $I_{\rm bias}$ is the constant source current across tunnel contact, whereas $\Delta V_{B_{\phi=0^\circ}}$ and $\Delta V_{B_{\phi=90^\circ}}$ have been defined earlier in Fig. 2(c). Hence, the $\Delta R_{\rm spin}$ represents the sum of the Hanle and inverted Hanle signal amplitudes, which is proportional to the spin

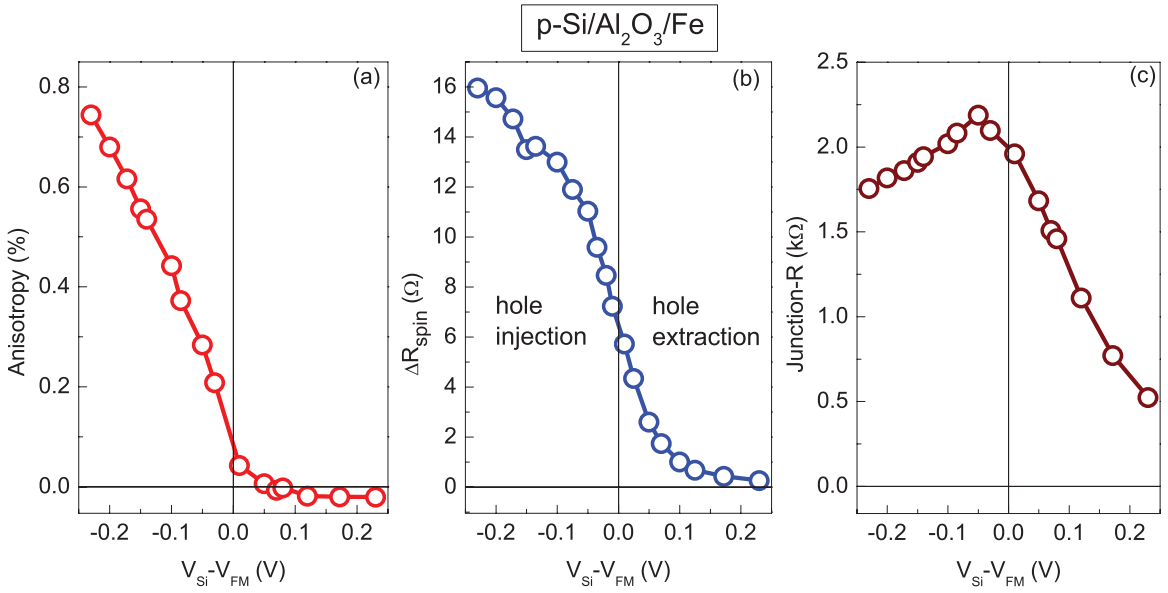

FIG. 6. (Color online) Bias dependence of (a) tunneling anisotropy and (b) spin resistance $\Delta R_{\text{spin}} = [\Delta V_{B_{\phi=0^\circ}} + \Delta V_{B_{\phi=90^\circ}}]/I_{\text{bias}}$, shown together with (c) junction resistance for p-Si/Al_2O_3/Fe tunnel junction. $\Delta V_{B_{\phi=0^\circ}}$ and $\Delta V_{B_{\phi=90^\circ}}$ have been defined in Fig. 2(c).

accumulation $\Delta\mu$. The spin resistance is asymmetric with respect to bias voltage, has a positive sign, and remains nonzero for all bias voltages. The measured voltage due to spin accumulation is proportional to the square of the TSP of the ferromagnet/insulator interface. As a result, the spin resistance ΔR_{spin} is always positive, independent of the sign of the spin accumulation or TSP. However, if there is a sign reversal of the TSP, the spin resistance must become zero at some bias voltage and become positive again. Since the observed spin resistance does not display a drop to zero, we conclude that the TSP does not change sign. In Fig. 6(c), we show the variation of the junction resistance with the bias voltage. We see that the junction resistance decays with bias voltage and more strongly for positive bias. When a bias is applied across the tunnel contact, electrons tunnel through the Al_2O_3 and Schottky barrier before reaching the bulk bands of the SC. Along negative bias, i.e., when $V < 0$, the depletion width in p-Si increases, while for $V > 0$, the width of the Schottky barrier is reduced. As a result, the tunneling probability is enhanced (reduced) for $V > 0$ ($V < 0$), giving rise to the asymmetry in the junction resistance.

In Fig. 7, we show a similar set of data for n-Si/Al_2O_3/Fe tunnel contacts. Compared to p-type Si, a different qualitative variation is observed for the tunneling anisotropy and spin

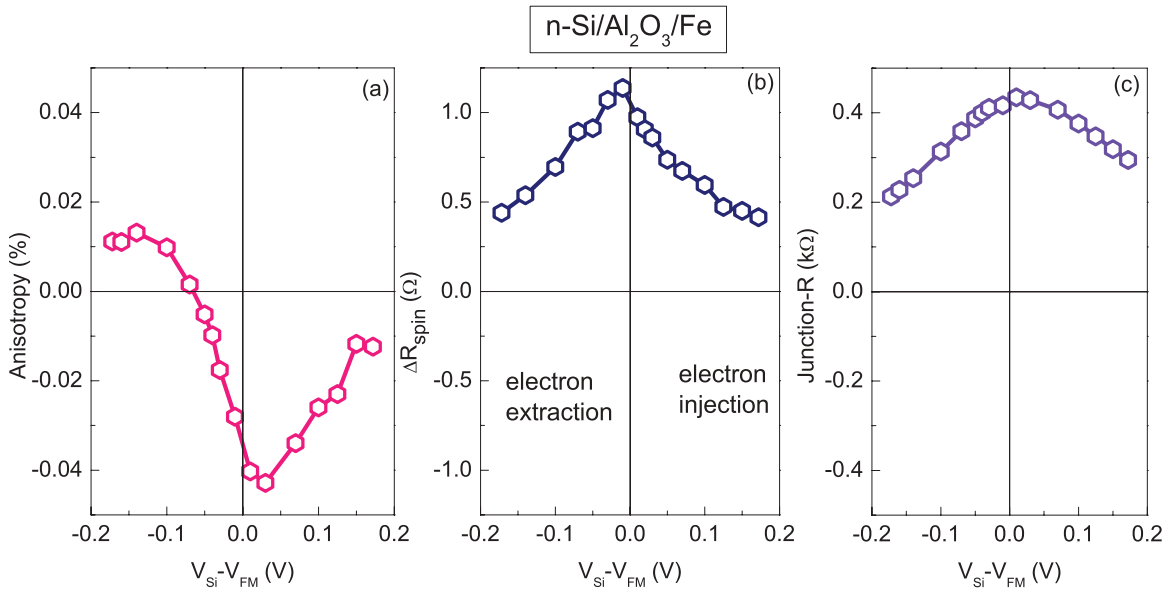

FIG. 7. (Color online) Bias dependence of the (a) tunneling anisotropy, (b) spin resistance ΔR_{spin}, and (c) junction resistance for n-Si/Al_2O_3/Fe tunnel junction.

resistance. Tunneling anisotropy [see Fig. 7(a)] has complex variation with bias voltage and it also changes sign with bias. However, the spin resistance ΔR_{spin} in Fig. 7(b), displays quite different behavior. It decreases monotonically and equally fast at $V > 0$ and $V < 0$ and does not change sign. It also has much less variation with bias compared to p-type Si with Fe. At negative bias (electron extraction), the junction resistance [see Fig. 7(c)] decreases slightly faster compared to positive bias (electron injection). The weak variation of tunnel resistance with bias is due to smaller depletion layer width for heavily doped n-Si, in combination with low work function of the Fe[27] (4.5 eV), which provides a lower Schottky barrier height for the tunnel contacts on n-Si.

2. *Tunnel contacts with Ni*

Figure 8 displays the data for the tunnel contact on p-Si with Ni. Both the tunneling anisotropy (a) and ΔR_{spin} (b) decrease with bias voltage in approximately the same way and there is no sign reversal for the anisotropy. The tunneling anisotropy is always positive, meaning higher resistance for in plane field ($\phi = 90^{\circ}$). The spin resistance ΔR_{spin} and the tunneling anisotropy approach zero when the bias has reached a value of 172 mV. Thus we see that for tunnel contacts with p-Si and Ni, the tunneling anisotropy and spin resistance behave similarly. In Fig. 8(c), the junction resistance is shown. It decreases slowly at negative bias (hole injection), whereas at positive bias the decrease is more significant. However, the bias asymmetry of the junction resistance is weaker than for p-Si with Fe. The lower work function of the Fe[27] (4.5 eV) compared to Ni (5 eV) gives rise to a larger Schottky barrier for Fe on p-type Si. As a result, the bias asymmetry of the junction resistance is stronger for tunnel contacts on p-Si with Fe.

In Fig. 9, a similar data set for n-Si/Al_2O_3/Ni tunnel contacts is shown. The tunneling anisotropy [see Fig. 9(a)] decays almost equally fast at negative (electron extraction) and positive (electron injection) bias. It does not change sign in the bias range investigated. Qualitatively the spin-resistance decreases in both bias direction similar to the tunneling anisotropy. The junction resistance in Fig. 9(c) has typical variation with bias voltage, reducing relatively fast (slow) for negative (positive) bias. Tunnel contacts on n-Si with large work function of Ni (5 eV) have a larger Schottky barrier as compared to the contact with Fe (4.5 eV). Larger Schottky barrier height results in a larger asymmetry in current across the tunnel contacts. As a result, the asymmetry of junction resistance in Fig. 9(c) for contacts with Ni is larger than for contacts with Fe [see Fig. 7(c)].

IV. ANALYSIS AND DISCUSSION

In this section, we will first discuss one of the sources of tunnel anisotropy that is well understood and originates from shape anisotropy, causing the magnetization direction to deviate from the direction of the applied magnetic field. Then we will describe the fitting equation that contains terms related to the TAMR and an anisotropic spin accumulation giving rise to the tunneling anisotropy. The sources of an ASA, namely, the anisotropic TSP associated with ferromagnet/insulator interface and anisotropic spin relaxation time in Si, have been introduced earlier. We also discuss that by a suitable combination of tunnel contacts on n and p-Si with different FM (Fe or Ni), the different contributions to an ASA and to tunneling anisotropic magnetoresistance can be separated.

A. Anisotropic spin accumulation in Si due to Hanle spin precession

For a magnetic thin film, the shape anisotropy favours a magnetization direction parallel to the surface, i.e., within the film plane, whereas an external field of 50 kOe favours the magnetization to align with it. Consequently, the external field and magnetization are not perfectly aligned, but they are at

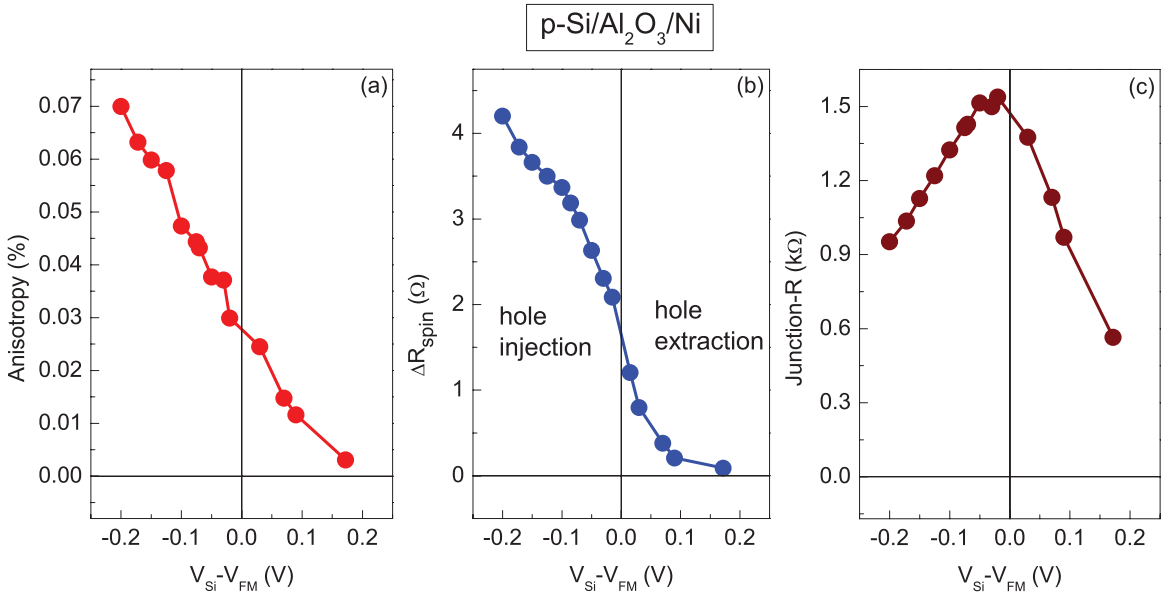

FIG. 8. (Color online) Bias dependence of the (a) tunneling anisotropy, (b) spin resistance, and (c) junction resistance for p-Si/Al_2O_3/Ni tunnel junction.

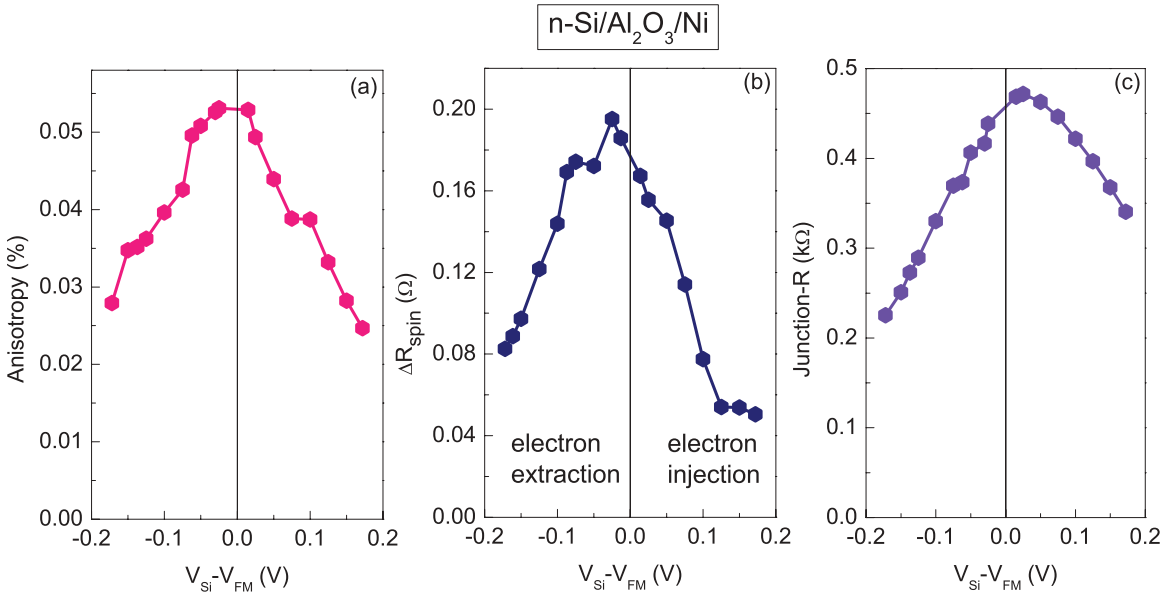

FIG. 9. (Color online) Bias dependence of the (a) tunneling anisotropy and (b) spin resistance shown together with the (c) junction resistance for n-Si/Al_2O_3/Ni tunnel junction.

angles ϕ and ϕ_M (see Fig. 1) with surface normal, respectively. The total energy of the magnetic layer consists of terms associated with the Zeeman energy and the demagnetizing energy due to shape anisotropy:

$$E_{\text{total}}(H,\phi,\phi_M) = -\mu_0 M_s H\cos(\phi-\phi_M) - \tfrac{1}{2}\mu_0 M_s^2 \sin^2(\phi_M), \quad (1)$$

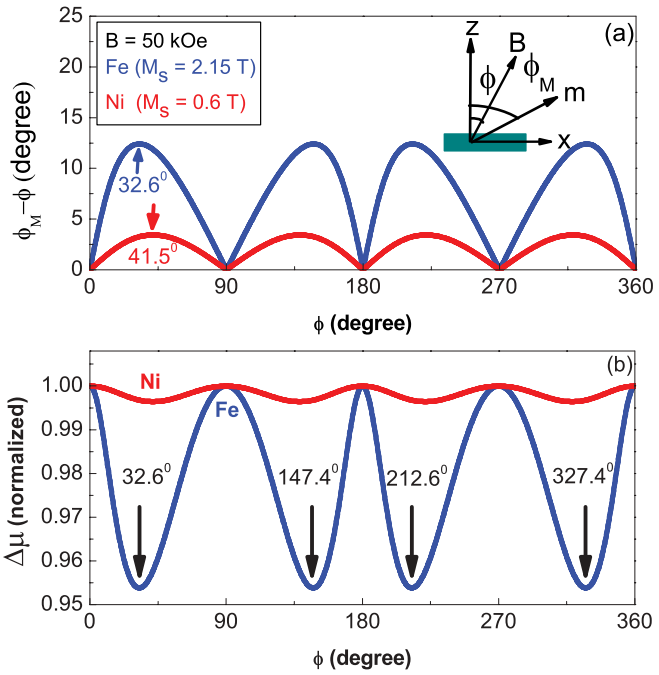

FIG. 10. (Color online) (a) The angle $\theta = \phi_M - \phi$ and (b) normalized spin accumulation $\Delta\mu$ vs field angle ϕ for Fe (blue) and Ni (red). In (a), at $\phi = 0^\circ$ and 90°, field and magnetization are aligned. For intermediate values of ϕ, the magnetization makes an angle of $\theta = (\phi_M - \phi)$ with the field. In (b), the spin accumulation has four pronounced minima (for Fe) at indicated ϕ values.

Here, μ_0, M_s, and H are magnetic permeability of vacuum, saturation magnetization, and external field, respectively. The orientation of the magnetization (ϕ_M) with respect to surface normal is determined by the energy minimization of the magnetic layer. Figure 10(a) shows $\phi_M - \phi$ as a function of field angle ϕ. At $\phi = 0^\circ$ and 90°, the field and magnetization are aligned perfectly. For intermediate values of ϕ, the difference $\theta = \phi_M - \phi$ has a maxima at $\phi = 32.6^\circ$ and 41.5° for Fe and Ni, respectively. We find that the difference $\phi_M - \phi$ is larger for Fe compared to Ni, which is attributed to larger shape anisotropy energy for Fe ($M_s = 2.15$ T) compared to Ni ($M_s = 0.6$ T). Due to misalignment of the magnetization with the field, the spins injected into silicon make an angle $\theta = \phi_M - \phi$ with the field, thereby leading to spin precession in Si even at a field of 50 kOe. The spin signal in terms of the angle θ between injected spins and magnetic field vector can be written as[25]

$$\Delta\mu \propto \left[\cos^2\theta + \frac{\sin^2\theta}{1+(\Omega_L\tau_s)^2}\right], \quad (2)$$

where τ_s is the spin relaxation time and $\Omega_L = g\mu_B B/\hbar$ is the Larmor frequency with g, μ_B, and $\hbar$ being the Lande's g factor, Bohr magneton and reduced Planck constant, respectively. In the limit $\Omega_L\tau_s \gg 1$ (due to large $B = 50$ kOe), the component of $\Delta\mu \perp$ B is completely suppressed. Therefore, in Eq. (2), the last term can be neglected. The net signal due to Hanle spin precession in the field will be

$$\Delta\mu = \Delta\mu^0(\cos^2\theta) = \Delta\mu^0\cos^2(\phi_M - \phi), \quad (3)$$

where $\Delta\mu^0$ is the spin signal when $\phi_M = \phi$, i.e, when magnetization and field are perfectly aligned. Figure 10(b) shows the calculated $\Delta\mu$ versus ϕ for Fe (blue) and Ni (red). There is a reduction of the spin signal with minima at $\phi = 32.6^\circ$, 147.4°, 212.6°, and 327.4° for the case of Fe. It is clear from Fig. 10(a) that for Fe the angular separation, $\phi_M - \phi$ is larger than for Ni. This in turn causes the suppression

[proportional to $\cos^2(\phi_M - \phi)$] of the signal in tunnel contacts with Fe to be more pronounced compared to those with Ni.

B. Fitting procedure

We found that the measured change in tunnel resistance, ΔR versus ϕ can be fit using the following equation:

$$\Delta R = A_0 + A_1 \cos(2\phi) + A_2 \cos(6\phi) + \Delta R_{\text{spin}} \cos^2(\phi_M - \phi), \quad (4)$$

where A_0 is a constant offset voltage, A_1 and A_2 are the fitting parameters. Reasonably good fits to the experimental data are obtained by considering the terms with twofold and sixfold symmetries. The prefactor[28] in the last term in Eq. (4) represents the spin accumulation (i.e., ΔR_{spin}), which is modulated by a factor $\cos^2(\phi_M - \phi)$, as noted in the previous section. The fits to the data using Eq. (4) are shown as solid lines in Figs. 3 and 5 for tunnel contacts with Fe and Ni, respectively. The parameters for the tunnel contacts with Fe are shown in Figs. 11 and 12, and for those with Ni in Fig. 13.

We first discuss the results for a tunnel contact on p-Si with Fe. At negative bias, A_1 is negative and reduces linearly as the bias voltage approaches zero. It changes sign at positive bias and thereafter does not vary much. Moving along positive bias (hole extraction), A_2 decays linearly up to 100 mV. Beyond that, it becomes very small and close to zero.

For the tunnel contact on n-Si with Fe, we find that A_1 changes sign and has a complex variation with bias voltage. A_2 reduces with increasing bias, and in the same way for positive and negative bias.

Figures 13(a) and 13(b) display the parameter A_1 for p-Si/Al_2O_3/Ni and n-Si/Al_2O_3/Ni tunnel contacts, respectively. Note that the data for tunnel contacts with Ni can be fitted without considering the terms with A_2 and ΔR_{spin} as the prefactor. As pointed out in the previous section, due to the small shape anisotropy energy of Ni, the last term in Eq. (4) can be neglected. For Ni contacts on p-type silicon [see Fig. 13(a)], A_1 is negative and increases for negative bias, whereas it decreases to zero for positive bias. For tunnel contact on n-Si [in Fig. 13(b)], A_1 is negative and decays almost symmetrically with bias voltage.

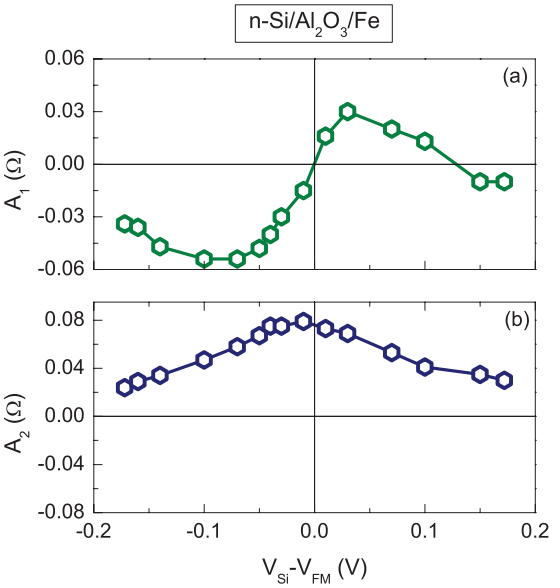

FIG. 12. (Color online) Fitting parameters (a) A_1 and (b) A_2 as a function of bias for n-Si/Al_2O_3/Fe tunnel contact.

C. Strategy for data interpretation

Here, we describe the criteria that will be adopted for interpreting the fitting results obtained above. We use the following two arguments for separating the different origins of the signal. (1) The spin resistance ΔR_{spin} is proportional to the spin accumulation $\Delta\mu$ in the Si. Therefore, if any

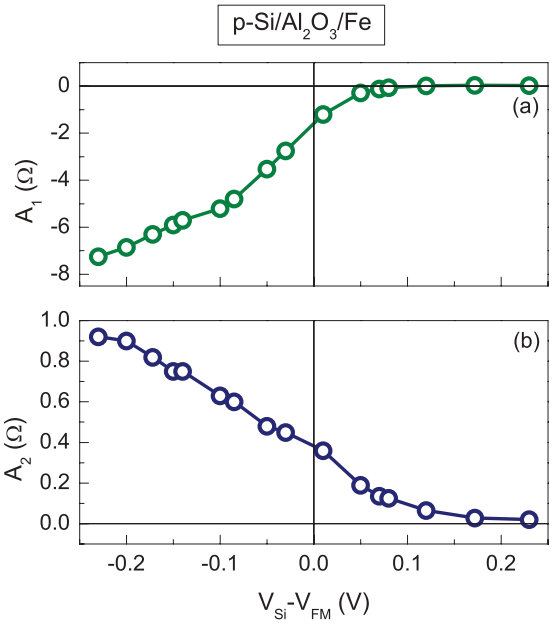

FIG. 11. (Color online) Fitting parameters (a) A_1 and (b) A_2 as a function of bias for p-Si/Al_2O_3/Fe tunnel contact.

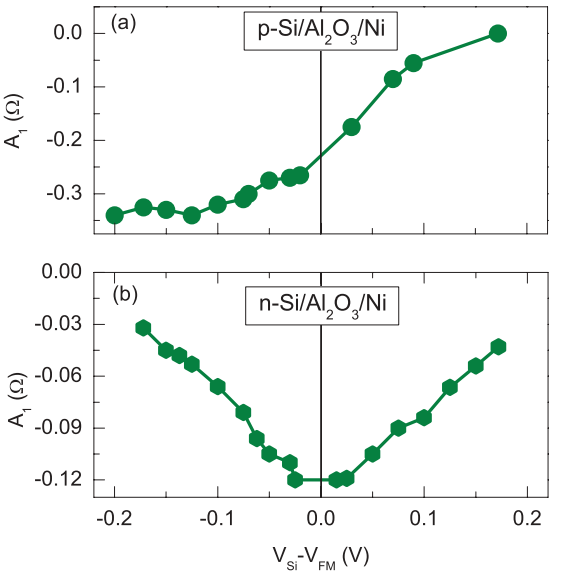

FIG. 13. (Color online) Parameter A_1 as a function of bias for (a) p-Si/Al_2O_3/Ni and (b) n-Si/Al_2O_3/Ni tunnel contacts.

one of the fitting parameters (i.e, A_1 or A_2) behaves as a function of V, in the same way as $\Delta R_{\rm spin}$ does, then we assume that the corresponding anisotropy comes from the anisotropic spin accumulation {term $V_{\rm ASA}(\Delta\mu(\phi))$}. The anisotropy in $\Delta\mu$ can come from either the anisotropic TSP of the ferromagnet/insulator interface or from an anisotropic spin-relaxation time τ_s in Si. These two sources can be distinguished as follows: (i) a contribution to the anisotropic τ_s inside the Si should be independent of the type of ferromagnet (Fe or Ni) used in the tunnel contacts. (ii) A contribution to the anisotropy from anisotropic TSP should be different for tunnel contacts with Fe and Ni. (2) If any one of the fitting parameter does not vary with V as the $\Delta R_{\rm spin}$ does, and the fitting parameter depends on the ferromagnet, then it is due to the TAMR.

D. Discussion

(1) Let us first consider the tunnel contacts with Fe. The last term in Eq. (4) with a pre-factor $\Delta R_{\rm spin}$ is dominant only in tunnel contacts with Fe. It comes from the misalignment of the magnetization and external field due to shape anisotropy of the thin magnetic film. This leads to four pronounced minima in the signal via the $\cos^2(\theta)$ term. Therefore this term partially accounts for the anisotropic spin accumulation inside Si.

(2) The term A_2 with sixfold symmetry is present in tunnel contacts with Fe and absent in those with Ni. Furthermore, A_2 has a bias variation similar to the spin resistance $\Delta R_{\rm spin}$, implying that this anisotropy originates from the spin accumulation. Since the anisotropy with sixfold symmetry is absent in Ni, a contribution due to anisotropic spin-relaxation time in Si is unlikely because it is not likely that contributions from TASP and anisotropic τ_s cancel at all bias voltages. We thus conclude that the sixfold anisotropy is due to anisotropy of $\Delta\mu$ arising from the anisotropic TSP of the magnetic tunnel contact.

(3) In tunnel contacts with n-Si and Fe, A_1 does not vary with V as $\Delta R_{\rm spin}$ does. Thus A_1 has a contribution from TAMR and this is responsible for the change in a sign of the tunneling anisotropy.

(4) The parameter A_1 (for p-Si) with twofold symmetry has a polarity that is opposite to the tunneling anisotropy and spin resistance. A part of A_1, along positive V, does not vary with V as $\Delta R_{\rm spin}$ does. This implies that A_1 has contributions due to anisotropic TSP of the FM and TAMR. The TAMR is responsible for the bias-induced inversion[21] of A_1, and gives rise to the experimentally observed change in tunneling anisotropy.

(5) Let us now consider the tunnel contacts on n and p-Si with Ni electrode for which only twofold anisotropy is observed. A_1 varies with bias voltage similar to the tunneling anisotropy and $\Delta R_{\rm spin}$, except that the polarity is opposite. This indicates that A_1 is due to the anisotropic spin accumulation $\Delta\mu$ in the Si. Furthermore, for tunnel contacts on n-Si with Fe and Ni, the bias variation of the tunneling anisotropy is different. Therefore the term A_1 and the tunneling anisotropy in these tunnel contacts must have a contribution from anisotropic TSP of the ferromagnet/tunnel barrier interface. However, note that the presence of an additional contribution from an anisotropic τ_s cannot be excluded.

TABLE I. Summary of the different sources of tunneling anisotropy identified in this work for different tunnel contacts.

Device	Fitting parameter	TAMR	ASA TASP	ASA τ_s
p-Si/Al_2O_3/Fe	A_1 (2ϕ)	yes	yes	possibly
	A_2 (6ϕ)	no	yes	no
n-Si/Al_2O_3/Fe	A_1 (2ϕ)	yes	yes	possibly
	A_2 (6ϕ)	no	yes	no
p-Si/Al_2O_3/Ni	A_1 (2ϕ)	no	yes	possibly
n-Si/Al_2O_3/Ni	A_1 (2ϕ)	no	yes	possibly

(6) For tunnel contacts on p-Si with Fe and Ni, the tunneling anisotropy and $\Delta R_{\rm spin}$ have similar variation with the bias voltage. The term A_1 with twofold symmetry decays similar to the tunneling anisotropy and $\Delta R_{\rm spin}$, but has opposite polarity. In tunnel contacts with Fe, the tunneling anisotropy and A_1 change sign along positive bias. This implies that for tunnel contact with Fe, the tunneling anisotropy and A_1 have contributions due to an ASA and TAMR. The TAMR is responsible for bias-induced inversion of the tunneling anisotropy and also A_1. The relative ratio $A_1/\Delta R_{\rm spin}$ for tunnel contacts on p-Si with Fe and Ni is $\sim$0.43 and $\sim$0.087, respectively. This difference implies that the observed anisotropy must have a contribution from the anisotropy of the TSP of the ferromagnet/tunnel barrier interface. However, the presence of an additional contribution from an anisotropic τ_s cannot be excluded.

A brief summary of the conclusions is given in Table I.

Let us finally compare the terms having twofold and sixfold symmetries with the literature. Metal magnetic tunnel junctions with one FM electrode have shown twofold symmetry of the anisotropy.[8] In addition, twofold and fourfold symmetries has been observed for MTJ's with two FM electrodes.[9] These features are attributed to TAMR due to anisotropic density of states at the tunnel interface. The sixfold anisotropy term we observe here is, as shown, due to the spin accumulation in the Si, and is therefore not observed in metal MTJ's. The precise origin of the sixfold term is still unclear and requires further investigations.

V. SUMMARY

We have observed out-of-plane tunneling anisotropy in Si/Al_2O_3/FM tunnel contacts. We find that different contributions to the tunneling anisotropy coexist. These can be distinguished using tunnel contacts on n- as well as p-type silicon and different ferromagnets (Fe and Ni). We found that an important source of anisotropy comes from the anisotropy of the tunnel spin polarization (TASP) of the ferromagnet/tunnel barrier interface. It makes the spin accumulation in the silicon dependent on the absolute orientation of the magnetization of the magnetic layer. We did not find any conclusive evidence for anisotropy of the spin lifetime in silicon, although the presence of a contribution from this mechanism cannot be excluded. The presence of tunneling anisotropic magnetoresistance (TAMR) in tunnel contacts with Fe gives rise to a bias-induced sign

inversion of the tunneling anisotropy. In comparison, tunnel contacts with Ni do not display such a sign inversion of the tunneling anisotropy.

ACKNOWLEDGMENTS

This work was financially supported by the Netherlands Foundation for Fundamental Research on Matter (FOM).

[1] M. Julliere, Phys. Lett. A **54**, 225 (1975).
[2] J. Fabian, A. Matos-Abiague, C. Ertler, P. Stano, and I. Žutić, Acta Phys. Slov. **57**, 565 (2007).
[3] C. Gould, C. Rüster, T. Jungwirth, E. Girgis, G. M. Schott, R. Giraud, K. Brunner, G. Schmidt, and L. W. Molenkamp, Phys. Rev. Lett. **93**, 117203 (2004).
[4] C. Rüster, C. Gould, T. Jungwirth, J. Sinova, G. M. Schott, R. Giraud, K. Brunner, G. Schmidt, and L. W. Molenkamp, Phys. Rev. Lett. **94**, 027203 (2005).
[5] A. Matos-Abiague and J. Fabian, Phys. Rev. B **79**, 155303 (2009).
[6] H. Saito, S. Yuasa, and K. Ando, Phys. Rev. Lett. **95**, 086604 (2005).
[7] T. Akiho, T. Uemura, M. Harada, K. ichi Matsuda, and M. Yamamoto, Jpn. J. Appl. Phys. **51**, 02BM01 (2012).
[8] B. G. Park, J. Wunderlich, D. A. Williams, S. J. Joo, K. Y. Jung, K. H. Shin, K. Olejník, A. B. Shick, and T. Jungwirth, Phys. Rev. Lett. **100**, 087204 (2008).
[9] L. Gao, X. Jiang, S.-H. Yang, J. D. Burton, E. Y. Tsymbal, and S. S. P. Parkin, Phys. Rev. Lett. **99**, 226602 (2007).
[10] H. Saito, S. Watanabe, Y. Mineno, S. Sharma, R. Jansen, S. Yuasa, and K. Ando, Solid State Commun. **151**, 1159 (2011).
[11] A. B. Shick, F. Máca, J. Mašek, and T. Jungwirth, Phys. Rev. B **73**, 024418 (2006).
[12] S. P. Dash, S. Sharma, R. S. Patel, M. P. de Jong, and R. Jansen, Nature (London) **462**, 491 (2009).
[13] R. Jansen, Nat. Mater. **11**, 400 (2012).
[14] Y. Ando, K. Hamaya, K. Kasahara, Y. Kishi, K. Ueda, K. Sawano, T. Sadoh, and M. Miyao, Appl. Phys. Lett. **94**, 182105 (2009).
[15] T. Sasaki, T. Oikawa, T. Suzuki, M. Shiraishi, Y. Suzuki, and K. Tagami, Appl. Phys. Express **2**, 053003 (2009).
[16] K. R. Jeon, B. C. Min, I. J. Shin, C. Y. Park, H. S. Lee, Y. H. Jo, and S. C. Shin, Appl. Phys. Lett. **98**, 262102 (2011).
[17] K. R. Jeon, B. C. Min, I. J. Shin, C. Y. Park, H. S. Lee, Y. H. Jo, and S. C. Shin, New J. Phys. **14**, 023014 (2012).
[18] S. P. Dash, S. Sharma, J. C. L. Breton, and R. Jansen, Proc. SPIE **7760**, 77600J (2010).
[19] R. Jansen, B. C. Min, S. P. Dash, S. Sharma, G. Kioseoglou, A. T. Hanbicki, O. M. J. van 't Erve, P. E. Thompson, and B. T. Jonker, Phys. Rev. B **82**, 241305 (2010).
[20] S. P. Dash, S. Sharma, J. C. Le Breton, J. Peiro, H. Jaffrès, J. M. George, A. Lemaitre, and R. Jansen, Phys. Rev. B **84**, 054410 (2011).
[21] J. Moser, A. Matos-Abiague, D. Schuh, W. Wegscheider, J. Fabian, and D. Weiss, Phys. Rev. Lett. **99**, 056601 (2007).
[22] A. Einwanger, M. Ciorga, U. Wurstbauer, D. Schuh, W. Wegscheider, and D. Weiss, Appl. Phys. Lett. **95**, 152101 (2009).
[23] M. Ciorga, A. Einwanger, U. Wurstbauer, D. Schuh, W. Wegscheider, and D. Weiss, Physica E **42**, 2673 (2010).
[24] N. Tombros, S. Tanabe, A. Veligura, C. Jozsa, M. Popinciuc, H. T. Jonkman, and B. J. van Wees, Phys. Rev. Lett. **101**, 046601 (2008).
[25] F. Meyer and B. P. Zakharchenya, *Optical Orientation* (Elsevier, Amsterdam, 1984).
[26] Y. A. Bychkov and E. I. Rashba, J. Phys. C **17**, 6039 (1984).
[27] H. B. Michaelson, J. Appl. Phys. **48**, 4729 (1977).
[28] In principle, the prefactor in the last term should include A_1 and A_2. However, during fitting, we observed that inclusion of these terms does not affect the previously extracted value of A_1 and A_2. Retaining ΔR_{spin} as a prefactor, makes the fitting procedure simple.